Journal of Pharmaceutical Analysis 14 (2024) 291–293

Contents lists available at ScienceDirect

Journal of Pharmaceutical Analysis

journal homepage: www.elsevier.com/locate/jpa

Short communication

N, S, Br co-doped carbon dots: One-step synthesis and fluorescent detection of 6-mercaptopurine in tablet

Qi Wang [a, *], Ying Cheng [a], Lifeng Ding [a], Shengling Li [a], Jie Zhang [a], Yulan Niu [a], Ziye Jing [b, **]

[a] Chemistry & Chemical Engineering Department, Taiyuan Institute of Technology, Taiyuan, 030008, China
[b] Department of Anesthesiology, First Hospital of Shanxi Medical University, Taiyuan, 030001, China

ARTICLE INFO

Article history:
Received 14 August 2023
Received in revised form
29 September 2023
Accepted 1 November 2023
Available online 4 November 2023

6-mercaptopurine (6-MP), a purine derivative (3,7-dihydro-purine-6-thione), has been utilized as an effective immunosuppressive drug for clinically treating leukemia and other autoimmune diseases [1]. 6-MP and its corresponding metabolites can suppress the function of RnaseH, and thus they are cytotoxic and threaten the human health [2]. Therefore, the accurate quantification of 6-MP is crucial. To date, researchers continue to expend considerable effort in developing 6-MP detection methods. Fluorescence analysis eliminates disadvantages, such as toxic solvents, expensive equipment, and complicated pretreatments, and has the advantages of high precision and sensitivity. Carbon dots (CDs) are a class of nanomaterials with a small size (below 10 nm) and excellent fluorescence performance [3]. CDs have been confirmed to have practical value in pharmaceutical analysis [4], demonstrating that it may be an effective tool for 6-MP detection. Therefore, in this study, nitrogen, sulfur, and bromine co-doped CDs (N, S, Br-CDs) are synthesized via a one-step hydrothermal method using bromophenol blue (BPB) and polyethyleneimine (PEI) as precursors. The heteroatoms are directly doped into the product during synthesis. In addition, the N, S, Br-CDs exhibited favorable fluorescence and is applied to detect 6-MP. The experimental details are shown in the Supplementary data. The transmission electron microscope (TEM) image (Fig. 1A) shows that CDs is a near spherical nanodot with a particle size below 10 nm. The insets show a lattice fringe with a spacing of 0.24 nm, which is consistent with the (110) lattice plane of graphene. The dynamic light scattering (DLS) analysis of the CDs (Fig. 1B) shows that the particles size is in the range of 2.33–5.61 nm and the average diameter is 3.77 nm. Fig. 1C shows the recorded ultraviolet-visible (UV-vis) absorption spectrum and fluorescence spectra. The CDs exhibit absorption at 250 and 350 nm, which are assigned to the $\pi \rightarrow \pi^*$ and $n \rightarrow \pi^*$ electron transitions, respectively, of the heteroatom-doped conjugated structure. Fig. S1 shows the fluorescence emission spectra of the CDs under different excitation and the three-dimensional (3D) fluorescence spectra is shown in Fig. 1D. The N, S, Br-CDs exhibited excitation-independent emission and the fluorescence intensity at 460 nm reached the maximum under 335 nm excitation.

Furthermore, the elemental composition and chemical state of the CDs were analyzed. The X-ray photoelectron spectroscopy (XPS) full scan spectrum (Fig. S2A) shows that the CDs contains C, O, N, S and Br. In particular, the C1s spectrum (Fig. S2B) was divided into three component peaks at 284.5, 285.6 and 286.2 eV originating from the C═C, C–N, and C–O bonds, respectively. In the O1s spectrum (Fig. S2C), two peak at 531.0 and 531.9 eV were detected, corresponding to the C═O and C–O–C/C–OH bonds, respectively. Two component peaks were detected at 399.2 and 401.2 eV in the N1s spectrum (Fig. S2D), which are attribute to the C–N and N–H bonds, respectively. Two component peaks were observed at 67.8 and 70.1 eV in the Br3d spectrum (Fig. S2E), corresponding to the $Br3d_{5/2}$ and $Br3d_{3/2}$ species, respectively. The S2p spectrum of (Fig. S2F) exhibits a characteristic peak at 168.2 eV, which confirmed the presence of RSO_3^-.

By exploiting the favorable fluorescence of the N, S, Br-CDs, the possibility of fluorescence detection of 6-MP was anticipated. Fig. 2A shows the recorded fluorescence emission spectra of the N, S, Br-CDs before and after introduction of 6-MP. The fluorescence intensity declined significantly after 6-MP addition. The clear decrease in the color of the fluorescence (insets photos) further demonstrates the fluorescence quenching.

To verify the underlying mechanism of fluorescence quenching, the fluorescence lifetime of the N, S, Br-CDs with or without 6-MP was measured. The corresponding fluorescence decay spectra are shown in Figs. 2B and C, and the fitted lifetime data are listed in Table S1. The fluorescence lifetime of CDs before and after 6-MP are 4.19 and 4.02 ns, respectively. The relatively unchanged

Peer review under responsibility of Xi'an Jiaotong University.
* Corresponding author.
** Corresponding author.
E-mail addresses: wangq@tit.edu.cn (Q. Wang), 13466854932@sohu.com (Z. Jing).

https://doi.org/10.1016/j.jpha.2023.11.001

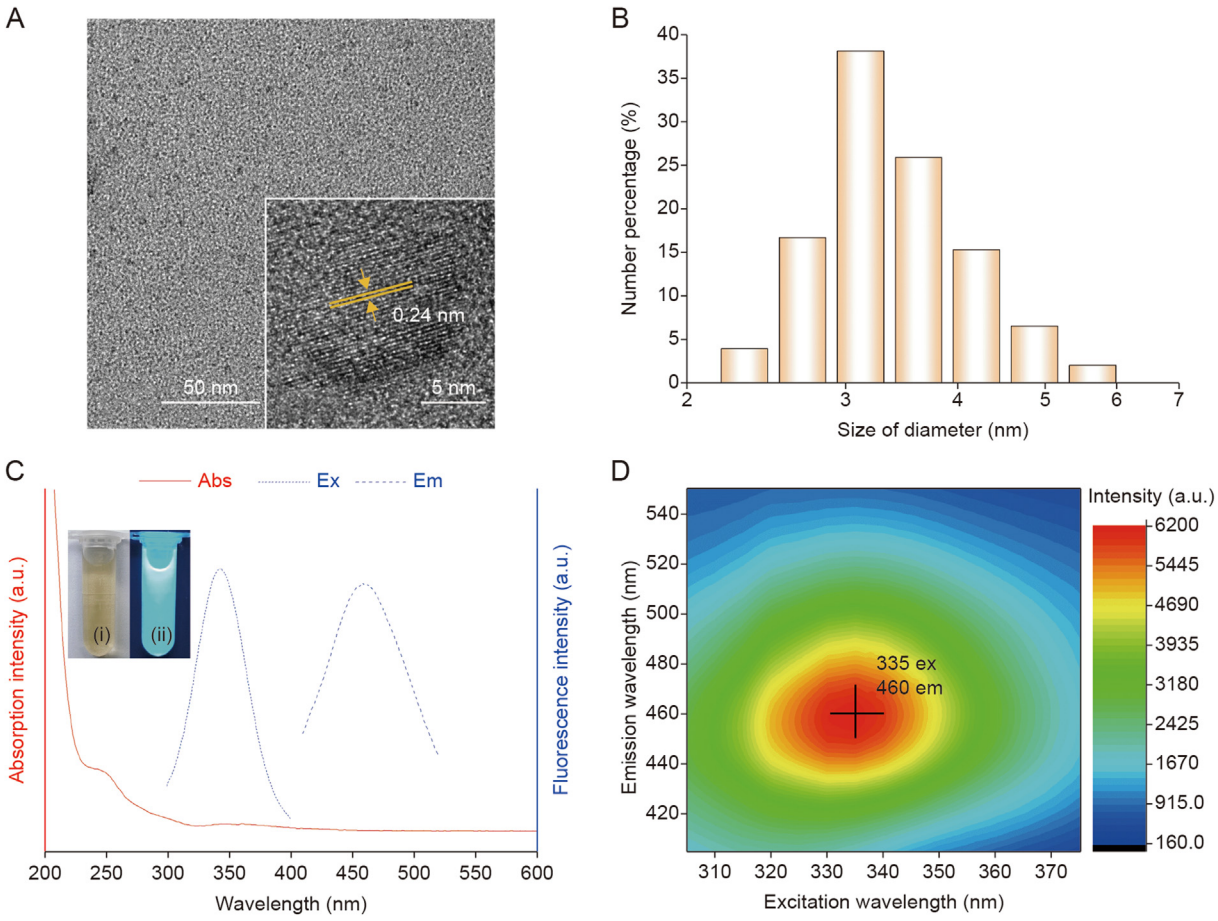

Fig. 1. The morphology, size and spectral properties of the N, S, Br-carbon dots (CDs). (A) The transmission electron microscope (TEM) and high-resolution transmission electron microscope (HRTEM) images of the N, S, Br-CDs. (B) The size distribution of the N, S, Br-CDs. (C) The ultraviolet-visible (UV-vis) absorption (red), fluorescence excitation and emission (blue) spectra of the N, S, Br-CDs. The insets are photos of N, S, Br-CDs solution under sunlight (i) and UV light illumination (ii). (D) The three-dimensional (3D) fluorescence spectra of the N, S, Br-CDs.

fluorescence lifetime revealed a static quenching effect (SQE) [5]. Furthermore, the UV-vis absorption spectrum of 6-MP and the fluorescence excitation spectrum of the N, S, Br-CDs were recorded and compared (Fig. 2D). A broad spectral overlay (shadow) was observed between the two spectra. The 335 nm excitation wavelength of the N, S, Br-CDs was in the absorption range of 6-MP, which promoted fluorescence quenching via inner filter effect (IFE) [5]. Therefore, the observed fluorescence quenching is concluded to be owing to the combination of SQE and IFE.

To achieve the optimal analytical sensitivity, the detection parameters were evaluated (Fig. S3). The time-dependent fluorescence intensity of the N, S, Br-CDs and N, S, Br-CDs + 6-MP were recorded (Fig. S3A). Considering the photobleaching of the CDs, the difference of fluorescence intensity (ΔF) was used to evaluate the quenching effect and the optimal time of 20 min was selected. In addition, the fluorescence quenching at pH values 11 and 13 were recorded, as shown in Figs. S4 and S5, respectively, and the pH of the detection system was investigated (Fig. S3B), demonstrating an optimal pH of 12.

Under these optimal detection conditions, the linear relationship between the 6-MP concentrations and the fluorescence quenching degree (F_0/F) was fitted (Fig. 2E), exhibiting a linear range of 8−300 μmol/L. The equation of the calibration curve was $Y = 0.9846 + 0.00256X$ ($R^2 = 0.9954$), where X is the 6-MP concentration (μmol/L) and Y represents F_0/F. The limit of detection (LOD) was 3.52 μmol/L (3σ). The fluorescence responses of potential coexisting compounds and other purines were evaluated (Figs. S6 and S7). The other species showed no response to the N, S, Br-CDs, demonstrating the excellent selectivity of the method. Furthermore, the developed method was applied to the analysis of real samples. A 6-MP-containing pharmaceutical tablet was selected as the real sample and standard addition method was performed. The detection results are listed in Table S2. The 6-MP content in the sample is 19.55 μmol/L and the recovery is in the range of 96.53 %–105.12 %. Compared with other state-of-the-art technologies (Table S3), this method possesses a wide linear range and improved detection accurate. According to the sample preparation process, dilution ratio and mass conversion, the 6-MP content in the tablet was calculated to be 0.27 mg/mg, which is similar to the labelled amount (50 mg/200 mg). These satisfactory results conformed the reliability of the method and practicability of the N, S, Br-CDs for 6-MP detection.

In summary, the N, S, Br co-doped CDs were synthesized using a facile hydrothermal process by direct doping with heteroatoms. Based on the favorable fluorescence of the as-synthesized N, S, Br-CDs, a novel fluorescent detection method for 6-MP was established. The fluorescence intensity of the N, S, Br-CDs was quenched by 6-MP via SQE and IFE. Therefore, quantitative analysis of 6-MP was achieved. In addition, the developed method was further applied to the analysis of pharmaceutical tablet. Although the LOD and analysis time require further improvements, the performance of the method met the requirements for the detection of 6-MP in real samples. Therefore, the N, S, Br-CDs is a promising tool for pharmaceutical analysis.

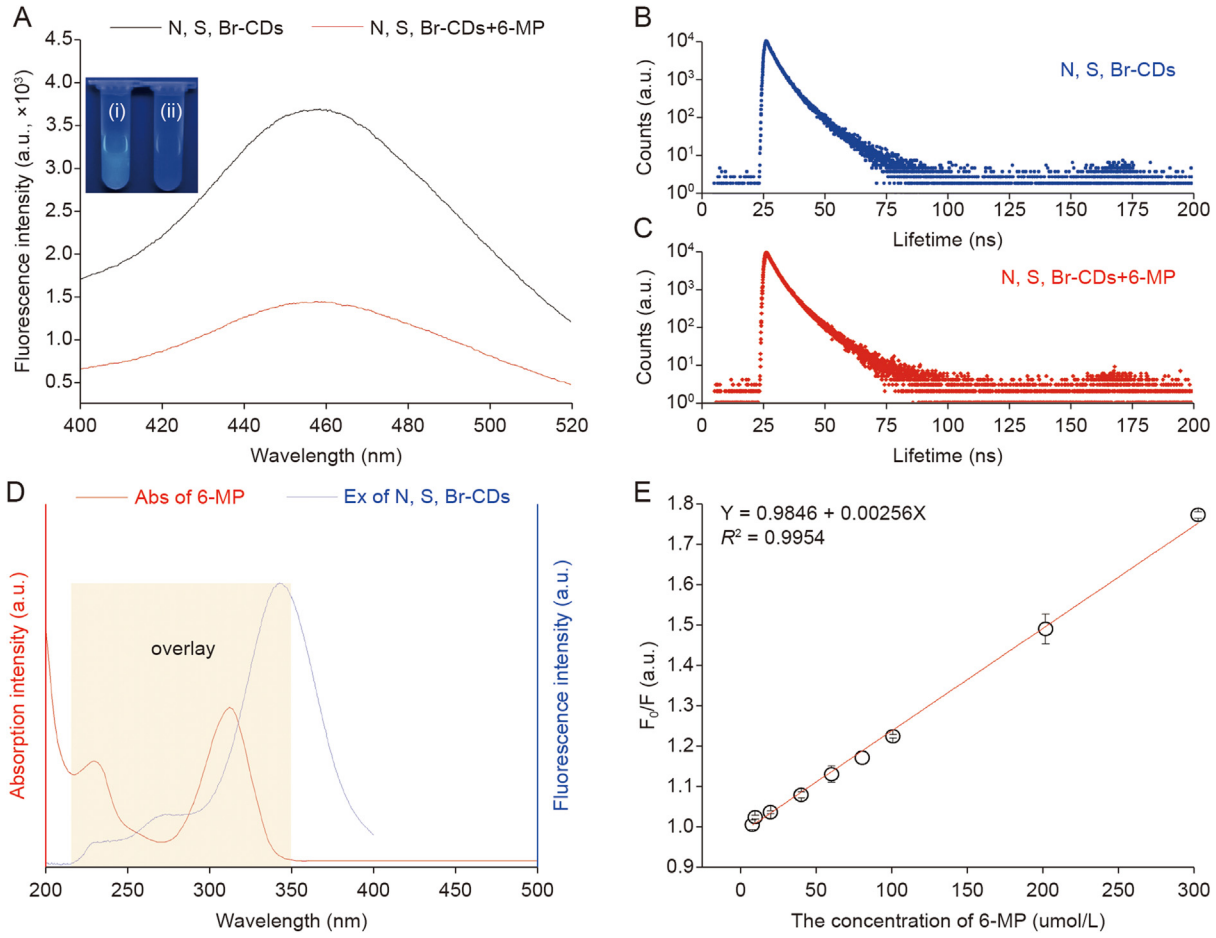

Fig. 2. The fluorescence detection performance and mechanism of the N, S, Br-carbon dots (CDs). (A) The fluorescence spectra of the N, S, Br-CDs in the absence (i, black) and presence (ii, red) of 6-mercaptopurine (6-MP). Insets: corresponding photos under 254 nm illumination. (B, C) The fluorescence decay of the (B) N, S, Br-CDs and (C) N, S, Br-CDs + 6-MP. (D) The spectra overlay of the ultraviolet-visible (UV-vis) absorption spectrum (red) of 6-MP and the fluorescence excitation spectrum (blue) of the N, S, Br-CDs. (E) The linear calibration curve for 6-MP detection through fluorescent quenching.

CRediT author statement

Qi Wang: Investigation, Data curation, Formal analysis, Methodology, Funding acquisition, Writing - Original draft preparation, Reviewing and Editing; **Ying Cheng**, **Lifeng Ding**, **Shengling Li**, and **Jie Zhang:** Investigation, Data curation, Formal analysis; **Yulan Niu:** Supervision, Conceptualization, Funding acquisition; **Ziye Jing:** Supervision, Conceptualization, Methodology.

Declaration of competing interest

The authors declare that there are no conflicts of interest.

Acknowledgments

The authors would like to thank the financial support of Taiyuan Institute of Technology Scientific Research Initial Funding, China (Grant No.: 2022KJ058), the Basic Research Project of Shanxi Province, China (Project No.: 202203021212331), the Scientific and Technological Innovation Programs of Higher Education Institutions in Shanxi, China (Program Nos.: 2022L529 and 2022L532), and the Fund for Shanxi "1331" Project, China.

Appendix A. Supplementary data

Supplementary data to this article can be found online at https://doi.org/10.1016/j.jpha.2023.11.001.

References

[1] C.L. Dieck, G. Tzoneva, F. Forouhar, et al., Structure and mechanisms of NT5C2 mutations driving thiopurine resistance in relapsed lymphoblastic leukemia, Cancer Cell 34 (2018) 136–147.e6.
[2] J.A. Nelson, J.W. Carpenter, L.M. Rose, et al., Mechanisms of action of 6-thioguanine, 6-mercaptopurine, and 8-azaguanine, Cancer Res. 35 (1975) 2872–2878.
[3] Z. Kang, B. Yang, M. Prato, Carbon nanodots: Nanolights illuminating a bright future, Small 19 (2023), e2304703.
[4] R. Ding, Y. Chen, Q.S. Wang, et al., Recent advances in quantum dots-based biosensors for antibiotics detection, J. Pharm. Anal. 12 (2022) 355–364.
[5] F. Zu, F. Yan, Z. Bai, et al., The quenching of the fluorescence of carbon dots: A review on mechanisms and applications, Microchim. Acta 184 (2017) 1899–1914.